JOURNAL OF BACTERIOLOGY, Apr. 2007, p. 2988–2995 Vol. 189, No. 8
0021-9193/07/$08.00+0 doi:10.1128/JB.01731-06

Intermolecular Forces and Enthalpies in the Adhesion of *Streptococcus mutans* and an Antigen I/II-Deficient Mutant to Laminin Films[▽]

Henk J. Busscher,[1] Betsy van de Belt-Gritter,[1] Rene J. B. Dijkstra,[1] Willem Norde,[1,2] Fernanda C. Petersen,[3] Anne A. Scheie,[3] and Henny C. van der Mei[1]*

Department of Biomedical Engineering, University Medical Center Groningen, and University of Groningen, Antonius Deusinglaan 1, 9713 AV Groningen, The Netherlands[1]; Laboratory of Physical Chemistry and Colloid Science, Wageningen University, P.O. Box 8038, 6700 EK Wageningen, The Netherlands[2]; and Department of Oral Biology, Faculty of Dentistry, University of Oslo, N0316 Oslo, Norway[3]

Received 10 November 2006/Accepted 29 January 2007

The antigen I/II family of surface proteins is expressed by most oral streptococci, including *Streptococcus mutans*, and mediates specific adhesion to, among other things, salivary films and extracellular matrix proteins. In this study we showed that antigen I/II-deficient *S. mutans* isogenic mutant IB03987 was nearly unable to adhere to laminin films under flow conditions due to a lack of specific interactions (0.8×10^6 and 1.1×10^6 cells cm^{-2} at pH 5.8 and 6.8, respectively) compared with parent strain LT11 (21.8×10^6 and 26.1×10^6 cells cm^{-2}). The adhesion of both the parent and mutant strains was slightly greater at pH 6.8 than at pH 5.8. In addition, atomic force microscopy (AFM) experiments demonstrated that the parent strain experienced less repulsion when it approached a laminin film than the mutant experienced. Upon retraction, combined specific and nonspecific adhesion forces were stronger for the parent strain (up to −5.0 and −4.9 nN at pH 5.8 and 6.8, respectively) than for the mutant (up to −1.5 and −2.1 nN), which was able to interact only through nonspecific interactions. Enthalpy was released upon adsorption of laminin to the surface of the parent strain but not upon adsorption of laminin to the surface of IB03987. A comparison of the adhesion forces in AFM with the adhesion forces reported for specific ligand-receptor complexes resulted in the conclusion that the number of antigen I/II binding sites for laminin on *S. mutans* LT11 is on the order of 6×10^4 sites per organism and that the sites are probably arranged along exterior surface structures, as visualized here by immunoelectron microscopy.

Streptococcus mutans is a commensal organism found in the human oral cavity (29). Its prevalence in dental plaque is associated with dental caries (25). However, upon dental treatment the organism may enter the bloodstream, which can result in infectious endocarditis. Most oral streptococci, including *S. mutans*, *Streptococcus sobrinus*, *Streptococcus gordonii*, and *Streptococcus intermedius*, express a family of structurally and antigenically related surface proteins termed antigen I/II with molecular masses ranging from 160 to 215 kDa (13, 21, 23, 30, 32). From the N terminus, the polypeptide has an amino-terminal signal peptide, an alanine-rich repeat unit, a variable region, a proline-rich repeat region, a carboxy-terminal wall- and membrane-spanning region, and an LPXTG wall anchor motif (19, 38). In *S. mutans*, antigen I/II plays an important role in streptococcal binding to salivary films and extracellular matrix proteins like fibronectin, laminin, collagen type I, and fibrinogen (3, 22). Studies in a parallel plate flow chamber (33) demonstrated that the ability of an antigen I/II isogenic mutant of *S. mutans* (IB03987) to adhere to salivary films under moderate shear conditions was reduced by 90% compared to the ability of the wild type (LT11) to adhere. No such conclusive studies have been performed to examine the abilities of these strains to adhere to laminin films. Laminins belong to a family of glycoproteins that provide an integral part of the scaffolding of basement membranes in almost every animal tissue. Each laminin is a heterotrimer assembled from α-, β-, and γ-chain subunits secreted and incorporated into cell-associated extracellular matrices (8). Laminin is a cross-shaped molecule with one leg longer than the other three and an unreduced molecular mass of 900 kDa.

Wild-type strain LT11 and mutant strain IB03987 were similarly hydrophilic based on water contact angles (38° and 30°, respectively) and had comparable negative surface charges, although LT11 had an isoelectric point around pH 2, whereas IB03987 was still negatively charged at pH 2 (33). However, other workers have reported that cell surface hydrophobicity, as determined by adhesion to hydrophobic ligands, is reduced in *S. mutans* isogenic mutants deficient in antigen I/II (16, 26, 31), but this may be because adhesion to hydrophobic ligands is essentially determined by an interplay of hydrophobic, electrostatic, and structural interactions.

In the past, microbial adhesion to surfaces has been described to be either specific or nonspecific, and the approach used by researchers has been largely dependent on their background. Physicochemists have usually examined microbial adhesion as a result of macroscopic interactions, as expressed by

* Corresponding author. Mailing address: Department of Biomedical Engineering, University Medical Center Groningen and University of Groningen, Antonius Deusinglaan 1, 9713 AV Groningen, The Netherlands. Phone: 31 50 3633140. Fax: 31 50 3633159. E-mail: h.c.van.der.mei@med.umcg.nl.

▽ Published ahead of print on 2 February 2007.

cell surface hydrophobicity and charge, whereas biochemists have preferred a more microscopic approach based on specific ligands and receptors. However, the distinction between the two approaches may not be as great as it seems, as it has been shown that microscopic, specific interactions are a result of the same physicochemical interaction forces that dominate macroscopic adhesion (5). Moreover, specific and nonspecific forces always operate in concert. Unfortunately, it took until the introduction of the atomic force microscope (AFM) in microbiology before the true nature of specific interactions could be experimentally assessed and compared with the nature of nonspecific forces.

AFM has been used extensively to detect forces in the nanonewton range between bacteria and substratum surfaces while operating under physiological conditions (14). Force measurements can be obtained by immobilizing bacteria on the AFM tip or cantilever, on a suitably prepared substratum surface, or on both, when forces between interacting bacteria are to be measured. Each method has advantages and disadvantages (40). Molecular determinants of *Escherichia coli* adhesion have been monitored by AFM, and the adhesive force has been found to be affected by the length of core lipopolysaccharides in the outer cell membrane (36). *Enterococcus faecalis* strains expressing aggregation substance (Agg) and adhering to biomaterial surfaces by means of positive cooperativity exhibited interaction forces between bacterial cells (about −2.5 nN) that were nearly twofold greater than the forces observed for a strain lacking Agg (adhesive force, −1.3 nN). The strong interaction forces between the strains with Agg decreased after adsorption of antibodies against Agg to about −1.2 nN, demonstrating the influence of specific antibodies on interaction forces between *E. faecalis* strains (41). Thus, these experiments indicated that it was possible that AFM could be used to experimentally distinguish between specific and nonspecific force components.

Whereas AFM operates at the nanometer level and can distinguish between different functional surface proteins, isothermal titration calorimetry (ITC) operates at a more macroscopic level. At a constant temperature and pressure, which is usually the case in biological systems, all interactions are determined by changes in the Gibbs energy (G) of a system. For a spontaneous process, the ΔG is negative. ΔG is composed of a change in enthalpy (H) and a change in entropy (S), as follows: $\Delta G = \Delta H - T\Delta S$, where T is the temperature (in Kelvin). The enthalpy tends to reach a minimum value reflecting the energetically most stable state, whereas the entropy strives for a maximum value corresponding to the highest degree of randomness. At a constant pressure, changes in the enthalpy can be determined by determining the heat exchange between the system and its environment. Many biological processes (e.g., assembly of viruses, protein folding, or biopolymer adsorption, as well as molecular interactions occurring at bacterial cell surfaces during adhesion) are characterized by strong enthalpy-entropy compensation (17); that is, they occur spontaneously by virtue of an increase in entropy that compensates for an unfavorable enthalpy effect or vice versa. Previously, ITC has seldom been used to study bacterial interactions, although it has recently been shown that coaggregation between oral actinomyces and streptococci is an exothermic process; i.e., heat is released upon coaggregation, resulting in a negative value for ΔH (34). Simultaneously, AFM indicated that a pair of coaggregating actinomyces and streptococci interacted with forces that were three- to fourfold higher than the forces observed for a pair of organisms lacking the ability to coaggregate, which interacted with a force of only 1 nN (35).

The aim of the present study was to analyze the role of *S. mutans* antigen I/II in adhesion to laminin-coated surfaces, using ITC and AFM. To do this, we first determined the adhesion of an *S. mutans* wild-type strain and of an antigen I/II isogenic mutant to laminin-coated glass slides in a parallel plate flow chamber under moderate shear conditions. Subsequently, the interaction forces between laminin-coated AFM tips and the *S. mutans* strains were compared using AFM, while the enthalpies of adsorption of laminin to the cell surfaces were compared using ITC.

MATERIALS AND METHODS

Bacterial strains and media. The *S. mutans* strains used in this study were *S. mutans* LT11, a highly transformable variant of UA159 (39), and an antigen I/II isogenic mutant inactivated at a single site, IB03987 (33). Isogenic mutant IB03987 was constructed by insertion of the suicide vector pSF151 carrying a kanamycin marker ligated to an internal antigen I/II target sequence into the chromosome of wild-type strain LT11. No reactivity with rabbit anti-antigen I/II immunoglobulin G (IgG) raised against purified *S. mutans* antigen I/II was observed after an immunoblotting analysis of cell extracts and supernatants of the mutant. The strains were stored at −80°C in brain heart infusion broth without (LT11) or with (IB03987) 500 μg ml^{-1} kanamycin (Oxoid, Basingstoke, United Kingdom) supplemented with 7% (vol/vol) dimethyl sulfoxide. Strains were also grown in brain heart infusion broth without or with 500 μg ml^{-1} kanamycin at 37°C in a CO_2 incubator.

Bacterial adhesion to a laminin film in a parallel plate flow chamber. Bacterial adhesion to the bottom glass plate of a parallel plate flow chamber was determined with a phase-contrast microscope coupled to a charge-coupled device-MXR camera and an image analyzer. Bacteria were cultured for 24 h, since we found previously by immunoblotting using antibodies against purified antigen I/II that the levels of expression of antigen I/II in *S. mutans* LT11 were similar at 24 h and in the late exponential phase. This culture was used to inoculate a second overnight culture, and the cultures were harvested by centrifugation, washed twice, and resuspended in adhesion buffer (2 mM potassium phosphate, 50 mM potassium chloride, 1 mM calcium chloride; pH 5.8 or 6.8) to a final concentration of 3×10^8 cells ml^{-1}. Laminin (from human placenta; Sigma Aldrich, Zwijndrecht, The Netherlands) was dissolved in adhesion buffer to a final concentration of 10 μg ml^{-1}. The bottom glass plate was coated with laminin for 2 h at room temperature. The experiments were performed at two pH values in order to study the influence of electrostatic interactions.

The bacterial flow rate was adjusted to 1.4 ml min^{-1} under the influence of hydrostatic pressure resulting in a shear rate of 10 s^{-1}. Live images were taken every 0.5 to 2 min during the first 30 min and thereafter at 10- to 30-min intervals up to 4 h, when the flow was stopped. The number of adhering bacteria was determined using the stored images. The initial deposition rate was calculated by determining the number of bacteria that adhered during the first 20 min per unit of time and area.

AFM. For AFM, bacteria were immobilized in an isopore polycarbonate membrane (20), while the AFM tips (NP probes; nominal tip radius, 20 nm; Veeco Inc., Woodbury, NY) were coated with a laminin film by immersion in a laminin solution (100 μg ml^{-1} in adhesion buffer, pH 5.8 or 6.8) for 30 min with the aid of a micromanipulator. All membranes with immobilized bacteria and laminin-coated AFM tips were used immediately for measurements.

AFM measurements were obtained at room temperature in adhesion buffer (pH 5.8 or 6.8) using an optical level microscope (Nanoscope III Digital Instruments, Santa Barbara, CA). An array of 32-by-32 force-distances curves with z displacements of 100 to 200 nm at z-scan rates of ≅10 Hz were collected over the entire field of view when a bacterium was imaged. The slopes of the retraction force curves in the region where the probe and sample were in contact were used to convert the voltage into cantilever deflection. Deflection was converted into force as previously described by other workers (14), using a nominal spring constant for the laminin-coated tips of 0.06 N m^{-1}, as determined by the method of Cleveland et al. (7). Force-distance curves taken over the top of each bacterium studied were analyzed in order to determine various characteristic param-

eters. Approach curves were fitted to an exponential function, where the interaction force (F) is described as $F = F_0 \exp(-d/\lambda)$, where F_0 is the force at zero separation between the interacting surfaces, d is the separation distance, and λ is the decay length of the interaction force. The retracting curves were used to generate adhesion maps. Adhesion maps were produced by using the strongest adhesive force detected during the retraction curve at each position as the value for adhesion and by plotting this value against the *x-y* position of each force-distance curve. From the adhesion maps a selected area of ~800 by 800 nm over the top of each bacterium was selected to generate an adhesion distribution histogram from which an average adhesion force was calculated for the adhesion between functionalized AFM tips and the bacterial cell surface for each experimental condition studied. Five different organisms were studied in each case.

ITC. The adsorption enthalpies of laminin with the two *S. mutans* strains were determined using a twin-type isothermal microcalorimeter (TAM 2277; Thermometric, Sweden). The calorimeter was placed in a temperature-controlled environment (20 ± 0.1°C), which resulted in a baseline stability of ±0.1 μW over 24 h (28). Experiments were performed isothermally at 25°C in 4-ml stainless steel ampoules. Four ampoules were connected with separate titration systems inside the microcalorimeter. The use of a twin-type microcalorimeter allowed measurement of the heat flowing from the reaction ampoule compared with the heat flowing from a reference ampoule. Signals were collected using the dedicated Digitam software (Thermometric, Sweden). The release of heat indicated that a process was exothermic and according to convention was associated with a negative value for ΔH.

Typically, all four reaction ampoules were filled with 1.5 ml of a streptococcal suspension (concentration, 5×10^9 cells per ml) that was constantly stirred (90 rpm) with a specially designed two-blade stirrer. The ampoules were allowed to equilibrate for 40 min within the calorimeter before data collection started. After equilibration, a stable heat flow was obtained, and 60 μl of a laminin solution (100 μg ml^{-1} in adhesion buffer, pH 5.8 or 6.8) was titrated into the reaction ampoules. Titration was done at a controlled rate of 2 μl s^{-1} via a stainless steel cannula connected to a syringe. In order to study possible saturation of binding sites, four portions of laminin were injected at 40-min intervals.

Electron microscopy. Overnight bacterial cultures were harvested and resuspended in phosphate-buffered saline to an optical density at 650 nm of 1. For immunogold labeling of thin sections we used the procedure described by Ayakawa et al. (1). The antibody used was rabbit anti-I/II IgG raised against purified antigen I/II from *S. mutans* OMZ 175 (a kind gift from J. Ogier) at a dilution of 1:1,500. Bovine serum albumin was included as the blocking agent.

RESULTS

***S. mutans* adhesion to laminin films.** Figure 1 shows a representative example of the kinetics of adhesion of *S. mutans* LT11 and IB03987 to laminin films in a parallel plate flow chamber. The bacterial adhesion kinetics were approximately linear during the first 20 to 30 min and then leveled off. The initial deposition rates for LT11 (1,957 ± 399 and 1,433 ± 178 cells cm^{-2} s^{-1} at pH 6.8 and 5.8, respectively) were significantly ($P < 0.005$, as determined by the Student t test) higher than the initial deposition rates for IB03987 (363 ± 250 and 137 ± 72 cells cm^{-2} s^{-1} at pH 6.8 and pH 5.8, respectively) and were slightly higher at pH 6.8 than at pH 5.8 ($P < 0.05$, as determined by the Student t test). Also, in the stationary phase (i.e., after 4 h), the numbers of LT11 organisms adhering (26.1 ± 0.9 and 21.8 ± 1.7 cells cm^{-2} s^{-1} at pH 6.8 and 5.8, respectively) were significantly greater than the numbers of IB03987 organisms adhering (1.1 ± 0.7 and 0.8 ± 0.4 cells cm^{-2} s^{-1} at pH 6.8 and 5.8, respectively), and again the numbers at pH 6.8 were slightly higher than the numbers at pH 5.8. Thus, these results clearly demonstrated that IB03987 was unable to adhere to laminin films compared with LT11.

Interaction forces between laminin and *S. mutans* cell surfaces. Figures 2 and 3 summarize the quantitative features of the approach and retraction force-distance curves, respectively, for LT11 and IB03987. Since all histograms showed a broad, non-Gaussian distribution of values for the repulsive force at contact, the repulsive force range, and the adhesion force, simple calculation of average values with standard deviations for the relevant parameters was not realistic. For this reason, we show the medians, modes, and ranges in Table 1. It is clear that the repulsive force upon approach (Fig. 2) was significantly ($P < 0.001$, as determined by the sign test for the median) smaller for LT11 (medians, 6.3 and 5.6 nN at pH 5.8 and 6.8, respectively) than for IB03987 (medians, 8.9 and 8.2 nN at pH 5.8 and 6.8, respectively) and that pH had no significant effect. The ranges of the repulsive forces upon approach were similar for both strains and pH values. For retraction (Fig. 3), the range analysis showed that no adhesion forces greater than −1.5 nN (at pH 5.8) and −2.1 nN (pH 6.8) were obtained for IB03987, whereas for LT11 the adhesion forces were as great as −5.0 nN and −4.9 nN at pH 5.8 and 6.8, respectively. The sign test for the median, however, revealed that the adhesion force for LT11 was significantly ($P < 0.001$) stronger than the adhesion force for IB03987 only at pH 6.8. Thus, the AFM results indicate that the repulsive forces that have to be overcome in order to allow an interaction between LT11 and laminin films are smaller than the repulsive forces that have to be overcome in order to allow an interaction between IB03987 and laminin. In addition, the interaction between LT11 and laminin films, once established, is more difficult to disrupt upon retraction than the interaction between IB03987 and laminin films. Moreover, these adhesion forces are stronger at pH 6.8 than at pH 5.8.

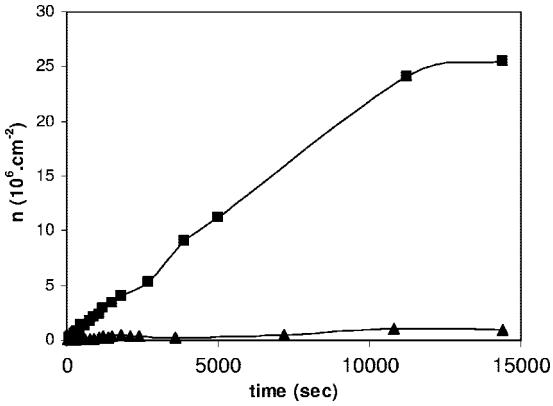

FIG. 1. Representative examples of the kinetics of adhesion of *S. mutans* LT11 (■) and IB03987 (▲) to laminin films in a parallel plate flow chamber at pH 6.8.

Enthalpies of adsorption of laminin to *S. mutans* cell surfaces. The enthalpy of adsorption of laminin to *S. mutans* cell surfaces was determined by injection of laminin into a suspension of *S. mutans* cells in adhesion buffer. This meant that the data had to be corrected for the enthalpy effect of dilution of the protein solution into a bacterium-free adhesion buffer. Multiple injections (up to four injections) of 60 μl of a 100-μg ml^{-1} laminin solution in adhesion buffer yielded enthalpy effects of −1,092 ± 236 and −38 ± 7 μJ per injection at pH 5.8 and 6.8, respectively. All adsorption enthalpies reported below were corrected by using these values.

Table 2 summarizes the adsorption enthalpy per bacterium for adsorption of laminin to the *S. mutans* cell surfaces. The enthalpy released upon consecutive injections of laminin into

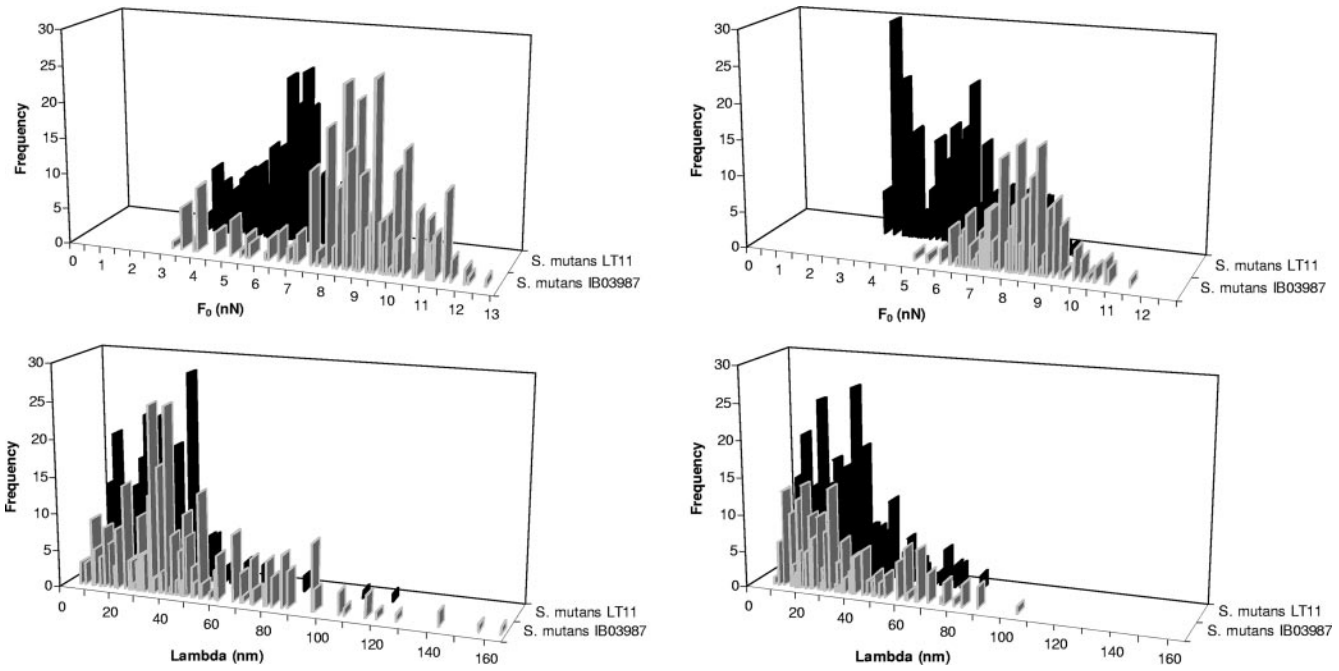

FIG. 2. Distribution of the repulsive force at contact (F_0) and its range (Lambda) for *S. mutans* LT11 and IB03987 for a laminin-coated AFM tip approaching cell surfaces. (Left panels) pH 5.8. (Right panels) pH 6.8. Each histogram was based on 200 to 300 force-distance curves, equally divided among five different bacteria.

LT11 suspensions was constant at pH 6.8, from which we concluded that the amounts of laminin injected were too small to saturate the cell surfaces at this pH. The initial injections of laminin at pH 5.8 were enthalpically more favorable than the initial injections at pH 6.8, but after the fourth injection a positive ΔH was observed, and cumulatively, the enthalpies released upon laminin injection into LT11 suspensions were similar at pH 6.8 and pH 5.8 (Fig. 4). Enthalpically, the adsorption of laminin to IB03987 was highly unfavorable compared with the adsorption of laminin to LT11 at both pH 5.8 and pH 6.8 ($P < 0.05$, as determined by the Student *t* test). For IB03987, however, the adsorption enthalpies per injection, as well as the cumulative adsorption enthalpy, were more favorable at pH 6.8 than at pH 5.8 ($P < 0.05$, as determined by the Student *t* test). Thus, ITC revealed favorable enthalpies for adsorption of laminin to LT11, but not for adsorption of laminin to IB03987. In addition, for IB03987 the adsorption enthalpies were more favorable at pH 6.8 than at pH 5.8.

Electron microscopy. Immunogold labeling was used to investigate the association of antigen I/II with the cell surface of *S. mutans* LT11 at the ultrastructural level. The gold particles appeared to be associated with structures exterior to the wild-type cell surface (Fig. 5a). No gold particles were associated with the antigen I/II-deficient mutant IB03987, supporting the specificity of the reaction (Fig. 5b).

DISCUSSION

In this study we showed that the antigen I/II-deficient *S. mutans* isogenic mutant IB03987 was nearly unable to adhere to laminin films under flow conditions compared with its parent strain, strain LT11. Antigen I/II was demonstrated to be located around 80 nm from the cell surface. Antigen I/II, however, is known to be anchored to the peptidoglycan layer through an LPXTG motif, which suggests that shed antigen I/II is associated with exterior cell surface structures. Since adhesion is a surface phenomenon, only the exterior antigen I/II is involved in adhesion and constitutes the binding sites, as discussed below. The adhesion of both the parent strain and the mutant was slightly greater at pH 6.8 than at pH 5.8. In agreement, AFM experiments demonstrated that the parent strain experienced less repulsion when it approached a laminin film than the mutant experienced, and it also exhibited stronger adhesion forces. Enthalpy was released upon adsorption of laminin to the surface of the parent strain but not upon adsorption to IB03987.

Adhesion to laminin films and interaction forces. Approach between two surfaces is always the first step in adhesion and occurs in the parallel plate flow chamber through convective diffusion of bacteria. Once the bacteria are close to a surface and within the range of the attractive interaction forces, adhesion occurs. In order for a bacterium to approach a surface close enough, electrosteric repulsion forces must be overcome. These repulsive forces have been associated with the repulsive forces that occur upon approach, as measured by AFM. The association between our adhesion results obtained in a parallel plate flow chamber and the repulsive forces observed upon approach of a laminin-coated AFM tip toward bacterial cell surfaces makes it clear that the presence of antigen I/II facilitates close approach of an organism to a laminin film.

Bacterial adhesion has been described as an interplay between specific and nonspecific interaction forces. The adhesion experiments which we carried out clearly demonstrated that there were no specific interactions between laminin films and

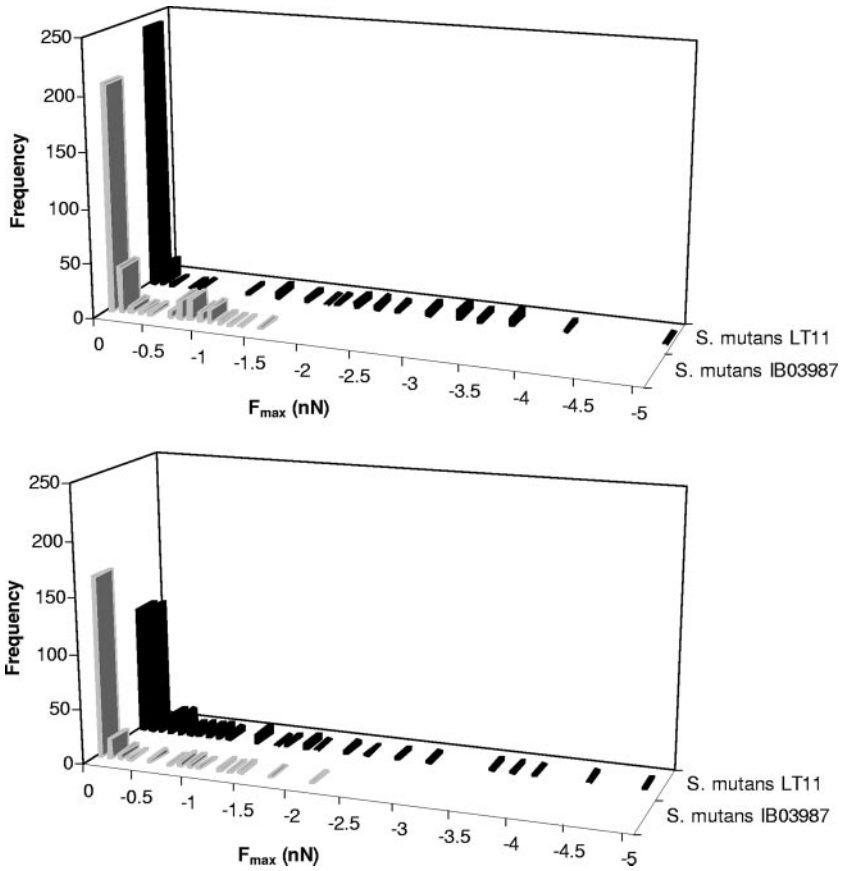

FIG. 3. Distribution of the adhesion force (F_{max}) for *S. mutans* LT11 and IB03987 for a laminin-coated AFM tip retracting from cell surfaces. (Top panel) pH 5.8. (Bottom panel) pH 6.8. Each histogram was based on 200 to 300 force-distance curves, equally divided among five different bacteria.

IB03987. The adhesion forces measured by AFM must therefore have been associated with nonspecific interactions and were −1.5 to −2.1 nN, which is two- to threefold less than the values obtained for the combined nonspecific and specific interactions between LT11 and laminin films. It is interesting that both similar ratios and similar absolute values for these interaction forces also occurred when workers compared specific and nonspecific interactions between (non)aggregating *E. faecalis* (41) and (non)coaggregating oral bacterial strains (35).

The adhesion forces between a laminin-coated AFM tip and the streptococcal cell surfaces can also be compared with the forces measured in an analogous way for highly specific, irreversible ligand-receptor pairs. For avidin-biotin complexes, adhesion forces ranging from 0.085 nN (avidin-iminobiotin) to 0.257 nN (streptavidin-biotin) per ligand-receptor pair were reported (27). The pairwise intermolecular forces for antigen-antibody interactions that have been reported range from 0.050 nN dor lysozyme-antilysozyme (4) and 0.063 nN for ferritin-antiferritin (15) to between 0.088 and 0.094 nN for human serum albumin and anti-human serum albumin (18). Thus, it is

TABLE 1. Medians, modes, and ranges of the distributions for the repulsive force at contact, the repulsive force range, and the adhesion force for the interactions of *S. mutans* LT11 and isogenic mutant IB03987 without antigen I/II with laminin-coated AFM tips in adhesion buffer at pH 5.8 and 6.8[a]

pH	Parameter	Repulsive force at contact (nN)		Repulsive force range (nm)		Adhesion force (nN)	
		LT11	IB03987	LT11	IB03987	LT11	IB03987
5.8	Median	6.3 (320)	8.9 (327)	28 (320)	40 (327)	0 (320)	0 (327)
	Mode	6.6	9.4	41	40	0	0
	Range	9.0	12.7	120	205	−5.0	−1.5
6.8	Median	5.7 (332)	8.3 (208)	28 (332)	29 (208)	−0.1 (332)	0 (208)
	Mode	3.7	8.3	32	31	−0.1	0
	Range	9.4	11.6	83	104	−4.9	−2.1

[a] All experiments were done five times with separately prepared laminin-coated AFM tips and different bacterial cultures, resulting in the numbers of distance curves indicated in parentheses.

TABLE 2. Adsorption enthalpies, corrected for the dilution of laminin into buffer, after consecutive injections of 60 μl of laminin (100 μg ml^{-1}) into suspensions of an *S. mutans* strain with antigen I/II (LT11) and an isogenic mutant without antigen I/II (IB03987) at a density of 5×10^9 cells ml^{-1}[a]

pH	Injection	Adsorption enthalpy (10^{-9} μJ per bacterium)	
		S. mutans LT11	*S. mutans* IB03987
5.8	1	−38 ± 35	13 ± 15
	2	−23 ± 24	17 ± 9
	3	−10 ± 33	38 ± 13
	4	9 ± 25	47 ± 11
	Cumulative	−61 ± 111	115 ± 26
6.8	1	−16 ± 3	1 ± 2
	2	−14 ± 7	−1 ± 3
	3	−18 ± 10	0 ± 3
	4	−15 ± 10	−1 ± 3
	Cumulative	−63 ± 29	−1 ± 10

[a] All experiments were done in adhesion buffer (pH 5.8 or 6.8) with five different bacterial cultures. The values are means ± standard deviations.

reasonable to assume that the pairwise interaction force between antigen I/II and laminin is between 0.05 and 0.10 nN. Since adhesion forces up to −5.0 nN have been measured for laminin and LT11, such a comparison suggests that between 50 and 100 ligand-receptor pairs are involved in the interaction between a laminin-coated AFM tip and the streptococcal cell surface. Considering that the radius of the AFM tip is approximately 25 nm and the radius of a bacterial cell is approximately 0.5 μm, it is estimated that a bacterial cell has between 4×10^4 and 8×10^4 antigen I/II binding sites.

The adhesion forces measured by AFM represent forced detachment, whereas during flow adhering organisms have to withstand detachment forces that are no higher than those that occur during adhesion. Thus, it is unlikely that the adhesion forces measured by AFM actually occur under the constant flow conditions in the parallel plate flow chamber. However, under environmental conditions, in which detachment forces fluctuate, the stronger adhesion forces for the strain possessing antigen I/II may be most relevant for the organisms to remain on a surface.

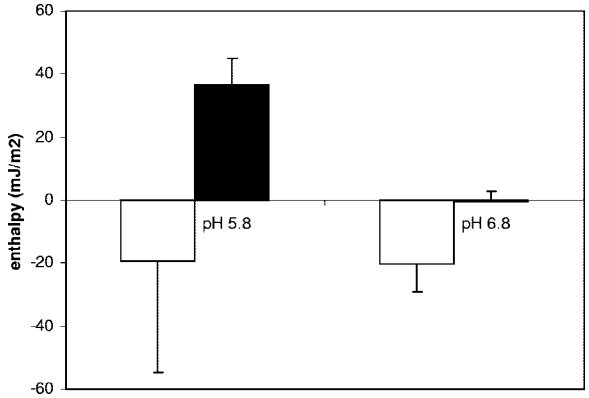

FIG. 4. Cumulative adsorption enthalpies after correction for the effects of laminin dilution and per unit of bacterial surface (mJ m^{-2}) after four injections of 60 μl of laminin (100 μg ml^{-1}) into suspensions (5×10^9 cells ml^{-1}) of an *S. mutans* strain with antigen I/II (LT11) (open bars) and an isogenic mutant without antigen I/II (IB03987) (solid bars) in adhesion buffer at pH 5.8 and pH 6.8. Experiments were carried out with three different bacterial cultures. The error bars indicate standard deviations.

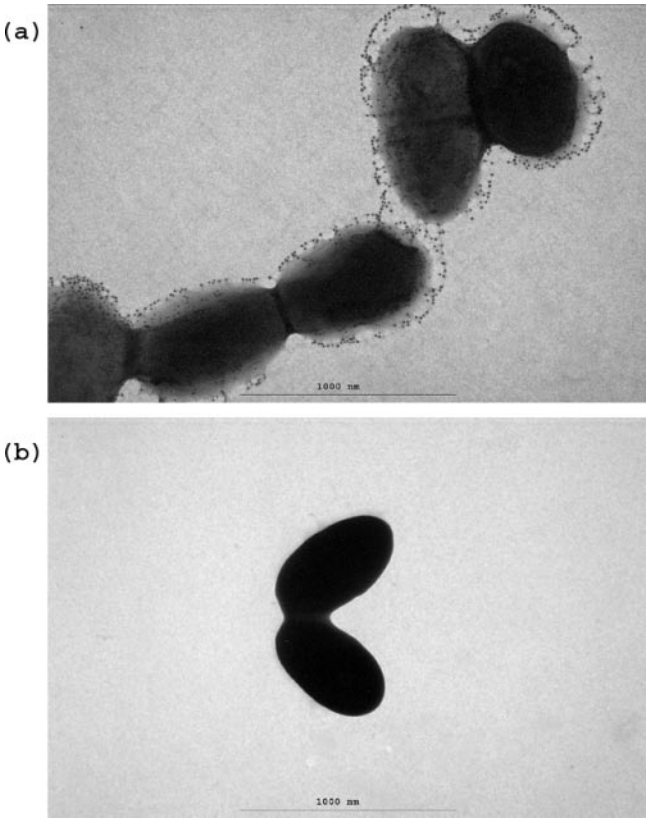

FIG. 5. Immunoelectron microscopy of gold-labeled antigen I/II of *S. mutans* LT11 (a) and mutant IB03987 (b).

Adhesion to laminin films and adsorption enthalpies. To our knowledge, ITC has never been used to measure the adsorption enthalpy between proteins and bacterial cell surfaces. Therefore, it is hard to judge whether the adsorption enthalpies measured were real, especially considering the large variations in the data (which are quite common in ITC, however). The enthalpies for adsorption of human serum albumin to various surfaces were as negative as −5 mJ m^{-2} (17). Recently, the enthalpies for adsorption of DNA to organic and inorganic clays have been measured (6). The enthalpies for adsorption of DNA to organic clays were endothermic, ranging from 8 to 19 mJ m^{-2}, and adsorption was entropy driven as a result of dehydration. Alternatively, DNA adsorption to inorganic clays was more extensive and exothermic, with a change in enthalpy of −1 to −15 mJ m^{-2} attributed to ligand exchange, hydrogen bonding, and electrostatic attraction. Although the examples described above do not include any specific interactions, the cumulative enthalpies for adsorption of laminin to LT11 (Fig. 4) are very comparable to those for adsorption of DNA to inorganic clays, suggesting that there are similar adsorption mechanisms involving ligand exchange, hydrogen bonding, and electrostatic attraction.

However, the laminin adsorption enthalpies per bacterium for LT11 can also be compared with the interaction enthalpies

in more specific systems. The interaction enthalpy for the irreversible, high-affinity binding of biotin to streptavidin is -2.2×10^{-16} mJ per molecule (26). Somewhat less-high-affinity interactions, like the interactions of concanavalin A with saccharides (10, 11) and with IgM (12), resulted in interaction enthalpies of -0.25×10^{-16} and -0.4×10^{-16} mJ per molecule, respectively; a value of -1.0×10^{-16} mJ per molecule has been obtained for the interaction enthalpy for IgG and IgM (37). Thus, the assumption that the interaction between antigen I/II and laminin is associated with an interaction enthalpy between -0.5×10^{-16} and -2.0×10^{-16} mJ per molecule appears to be reasonable. Comparison with the cumulative laminin adsorption enthalpy per bacterium measured in this study resulted in the conclusion that there must be between 3×10^5 and 13×10^5 antigen I/II binding sites per bacterium; however, in contrast to the AFM data, such a comparison is probably not valid for the ITC data. In nature, laminin never occurs in a dissolved state, and therefore it is likely that laminin dissolved during ITC has a different conformational state than laminin adsorbed to a surface, as in AFM.

Synthesis and conclusions. The adhesion of LT11 to laminin films in a parallel plate flow chamber was demonstrated to be much greater than the adhesion of IB03987. This is in line with the greater repulsion experienced by IB03987 when it approached a laminin-coated tip and the stronger adhesion forces measured for LT11 upon forced disruption of a laminin-coated tip from bacterial cell surfaces. The strong adhesion forces measured for LT11 are in line with the highly negative laminin adsorption enthalpies measured for LT11, suggesting that the antigen I/II binding with laminin involves attractive, short-range interactions between oppositely charged domains on the interacting ligands and receptors. The importance of attractive electrostatic interactions between bacteria and proteinaceous surfaces has been suggested previously (for instance, for the adhesion of *Treponema denticola* to red blood cells [9]).

Based on previously published data for the interaction forces between single ligand-receptor bonds, it has been calculated that about 6×10^4 antigen I/II binding sites must be present per LT11 cell. Assuming a projected area of 100 nm^2 per antigen I/II binding site, which is valid for a molecule like IgG (2), 3×10^4 sites would fully cover the bacterial cell surface. Distribution of about twofold more sites would require antigen I/II to bind to more than one laminin molecule or antigen I/II sites to be arranged along structural surface appendages on the cell surface. Supporting the latter suggestion, the presence of antigen I/II in a fibrillar fuzzy layer in *S. mutans* has been reported previously (1, 10, 24). An electron micrograph of immunogold-labeled antigen I/II on *S. mutans* LT11 confirmed that antigen I/II is located exterior to the wild-type cell surface and that the mutant is deficient in antigen I/II (Fig. 5).

In summary, this is the first time that the number of specific binding sites on a bacterial cell surface has been estimated based on AFM and ITC measurements. Our estimate seems realistic and provides an indication of the density of microscopic, specific sites involved in *S. mutans* adhesion to laminin films.

REFERENCES

1. **Ayakawa, G. Y., L. W. Boushell, P. J. Crowley, G. W. Erdos, W. P. McArthur, and A. S. Bleisweis.** 1987. Isolation and characterization of monoclonal antibodies specific for antigen P1, a major surface protein of mutans streptococci. Infect. Immun. **55:**2759–2767.
2. **Bagchi, P., and S. M. Birnbaum.** 1981. Effect of pH on the adsorption of immunoglobulin G on anionic poly(vinyl) model latex particles. J. Colloid Interface Sci. **83:**460–478.
3. **Beg, A. M., M. N. Jones, T. Miller-Torbert, and R. G. Holt.** 2002. Binding of *Streptococcus mutans* to extracellular matrix molecules and fibrinogen. Biochem. Biophys. Res. Commun. **298:**75–79.
4. **Berquand, A., N. Xia, D. G. Castner, B. H. Clare, N. L. Abbott, V. Dupres, Y. Adriaensen, and Y. F. Dufrene.** 2005. Antigen binding forces of single antilysozyme Fv fragments explored by atomic force microscopy. Langmuir **21:**5517–5523.
5. **Busscher, H. J., M. M. Cowan, and H. C. van der Mei.** 1992. On the relative importance of specific and non-specific approaches to oral microbial adhesion. FEMS Microbiol. Rev. **8:**199–209.
6. **Cai, P., Q. Huang, D. Jiang, X. Rong, and W. Liang.** 2006. Microcalorimetric studies on the adsorption of DNA by soil colloidal particles. Colloid Surf. B Biointerfaces **49:**49–54.
7. **Cleveland, J. P., S. Manne, D. Bocek, and P. K. Hansma.** 1993. A nondestructive method for determining the spring constant of cantilevers for scanning force microscopy. Rev. Sci. Instrum. **64:**403–405.
8. **Colognato, H., and P. D. Yurchenco.** 2000. Form and function: the laminin family of heterotrimers. Dev. Dynam. **218:**213–234.
9. **Cowan, M. M., F. H. M. Mikx, and H. J. Busscher.** 1994. Electrophoretic mobility and hemagglutination of *Treponema denticola* ATCC 33520. Colloids Surf. B Biointerfaces **2:**407–410.
10. **Cuisinier, F. J., J. P. Klein, and R. M. Frank.** 1990. Immunolabelling of SR protein and serotype polysaccharide in *Streptococcus mutans*. J. Gen. Microbiol. **136:**975–977.
11. **Dani, M., F. Manca, and G. Rialdi.** 1981. Calorimetric study of concanavalin A binding to saccharides. Biochim. Biophys. Acta **667:**108–117.
12. **Dani, M., F. Manca, and G. Rialdi.** 1982. Calorimetric study of the binding reaction of concanavalin A with immunoglobulins. Mol. Immunol. **19:**907–911.
13. **Demuth, D. R., Y. Duan, W. Brooks, A. R. Holmes, R. McNab, and H. F. Jenkinson.** 1996. Tandem genes encode cell-surface polypeptides SspA and SspB which mediate adhesion of the oral bacterium *Streptococcus gordonii* to human and bacterial receptors. Mol. Microbiol. **20:**403–413.
14. **Dufrêne, Y. F.** 2003. Recent progress in the application of atomic force microscopy imaging and force spectroscopy to microbiology. Curr. Opin. Microbiol. **6:**317–323.
15. **Harada, Y., M. Kuroda, and A. Ishida.** 2000. Specific and quantized antigen-antibody interaction measured by atomic force microscopy. Langmuir **16:**708–715.
16. **Harrington, D. J., and R. R. B. Russell.** 1993. Multiple changes in cell wall antigens of isogenic mutants of *Streptococcus mutans*. J. Bacteriol. **175:**5925–5933.
17. **Haynes, C. A., and W. Norde.** 1994. Globular proteins at solid/liquid interfaces. Colloids Surf. B Biointerfaces **2:**517–566.
18. **Idiris, A., S. Kidoaki, K. Usui, T. Maki, H. Suzuki, M. Ito, M. Aoki, Y. Hayashizaki, and T. Matsuda.** 2005. Force measurement for antigen-antibody interaction by atomic force microscopy using a photograft-polymer spacing. Biomacromolecules **6:**2776–2784.
19. **Jakubovics, N. S., N. Stromberg, C. J. van Dolleweerd, C. G. Kelly, and H. F. Jenkinson.** 2005. Differential binding specificities of oral streptococcal antigen I/II family adhesins for human or bacterial ligands. Mol. Microbiol. **55:**1591–1605.
20. **Kasas, S., and A. Ikai.** 1995. A method for anchoring round shaped cells for atomic force microscope imaging. Biophys. J. **68:**1678–1680.
21. **Kelly, C., P. Evans, L. Bergmeier, S. F. Lee, A. Progulske-Fox, A. C. Harris, A. Aitken, A. S. Bleiweis, and T. Lehner.** 1989. Sequence analysis of the cloned streptococcal cell surface antigen I/II. FEBS Lett. **258:**127–132.
22. **Koga, T., N. Okahashi, I. Takahashi, T. Kanamoto, H. Asakawa, and M. Iwaki.** 1990. Surface hydrophobicity, adherence, and aggregation of cell surface protein antigen mutants of *Streptococcus mutans* serotype c. Infect. Immun. **58:**289–296.
23. **LaPolla, R. J., J. A. Haron, C. G. Kelly, W. R. Taylor, C. Bohart, M. Hendricks, J. P. Pyati, R. T. Graff, J. K. Ma, and T. Lehner.** 1991. Sequence and structural analysis of surface protein antigen I/II (SpaA) of *Streptococcus sobrinus*. Infect. Immun. **59:**2677–2685.
24. **Lee, S. F., A. Progulske-Fox, G. W. Erdos, D. A. Piacentini, G. Y. Ayakawa, P. J. Crowley, and A. S. Bleiweis.** 1989. Construction and characterization of isogenic mutants of *Streptococcus mutans* deficient in major surface protein antigen P1 (I/II). Infect. Immun. **57:**3306–3313.
25. **Loesche, W. J.** 1986. Role of *Streptococcus mutans* in human dental decay. Microbiol. Rev. **50:**353–380.
26. **McBride, B. C., M. Song, B. Krasse, and J. Olsson.** 1984. Biochemical and immunological differences between hydrophobic and hydrophilic strains of *Streptococcus mutans*. Infect. Immun. **44:**68–75.
27. **Moy, V. T., E. L. Florin, and H. E. Gaub.** 1994. Intermolecular forces and energies between ligand and receptors. Science **266:**257–259.
28. **Nordmark, M. G., J. Laynez, A. Schön, J. Suurkuusk, and I. Wadsö.** 1984.

Design and testing of a new microcalorimetric vessel for use with living cellular systems and in titration experiments. J. Biochem. Biophys. Methods **10:**187–202.
29. **Nyvad, B., and M. Kilian.** 1990. Comparison of the initial streptococcal microflora on dental enamel in caries-active and in caries-inactive individuals. Caries Res. **24:**267–272.
30. **Ogier, J. A., M. Scholler, Y. Leproivre, A. Pini, P. Sommer, and J. P. Klein.** 1990. Complete nucleotide sequence of the sr gene from *Streptococcus mutans* OMZ 175. FEMS Microbiol. Lett. **56:**223–227.
31. **Okahashi, N., C. Sasakawa, M. Yoshikawa, S. Hamada, and T. Koga.** 1989. Molecular characterization of a surface protein antigen gene from serotype c *Streptococcus mutans*, implicated in dental caries. Mol. Microbiol. **3:**673–678.
32. **Petersen, F. C., S. Pasco, J. Ogier, J. P. Klein, S. Assev, and A. A. Scheie.** 2001. Expression and functional properties of the *Streptococcus intermedius* surface protein antigen I/II. Infect. Immun. **69:**4647–4653.
33. **Petersen, F. C., S. Assev, H. C. van der Mei, H. J. Busscher, and A. A. Scheie.** 2002. Functional variation of the antigen I/II surface protein in *Streptococcus mutans* and *Streptococcus intermedius*. Infect. Immun. **70:**249–256.
34. **Postollec, F., H. J. Busscher, T. G. van Kooten, H. C. van der Mei, and W. Norde.** 2004. Path-dependency of the interaction between co-aggregating and non-co-aggregating oral bacterial pairs—a thermodynamic approach. Colloids Surf. B Biointerfaces **37:**53–60.
35. **Postollec, F., W. Norde, J. de Vries, H. J. Busscher, and H. C. van der Mei.** 2006. Interactive forces between co-aggregating and non-co-aggregating oral bacterial pairs. J. Dent. Res. **85:**231–234.
36. **Razatos, A., Y. L. Ong, M. M. Sharma, and G. Georgiou.** 1998. Molecular determinants of bacterial adhesion monitored by atomic force microscopy. Proc. Natl. Acad. Sci. USA **95:**11059–11064.
37. **Rialdi, G., and S. Raffanti.** 1984. The use of flow calorimetry in antigen-antibody reactions. Immun. Lett. **7:**335–338.
38. **Seifert, T. B., A. S. Bleiweis, and L. J. Brady.** 2004. Contribution of the alanine-rich region of *Streptococcus mutans* P1 to antigenicity, surface expression, and interaction with the proline-rich repeat domain. Infect. Immun. **72:**4699–4706.
39. **Tao, L., T. J. MacAlister, and J. M. Tanzer.** 1993. Transformation efficiency of EMS-induced mutants of *Streptococcus mutans* of altered cell shape. J. Dent. Res. **72:**1032–1039.
40. **Vadillo-Rodriguez, V., H. J. Busscher, W. Norde, J. de Vries, R. J. B. Dijkstra, I. Stokroos, and H. C. van der Mei.** 2004. Comparison of atomic force microscopy interaction forces between bacteria and silicon nitride substrata for three commonly used immobilization methods. Appl. Environ. Microbiol. **70:**5441–5446.
41. **Waar, K., H. C. van der Mei, H. J. M. Harmsen, J. de Vries, J. Atema-Smit, J. E. Degener, and H. J. Busscher.** 2005. Atomic force microscopy study on specificity and non-specificity of interaction forces between *Enterococcus faecalis* cells with and without aggregation substance. Microbiology **151:**2459–2464.